energies

MDPI

Article

Neural Network Approach for Global Solar Irradiance Prediction at Extremely Short-Time-Intervals Using Particle Swarm Optimization Algorithm

Ahmed Aljanad [1,2,*], Nadia M. L. Tan [2,*], Vassilios G. Agelidis [2,3] and Hussain Shareef [4]

1 Department of Science, Technology, Engineering and Mathematics, American University of Afghanistan, Darul Aman 4001, Kabul, Afghanistan
2 Institute of Power Engineering, Universiti Tenaga Nasional, Kajang 43000, Selangor, Malaysia; vasagel@elektro.dtu.dk
3 Department of Electrical Engineering, Technical University of Denmark, 2800 Kongens Lyngby, Denmark
4 Department of Electrical Engineering, United Arab Emirates University, Al Ain 15551, Abu Dhabi, United Arab Emirates; shareef@uaeu.ac.ae
* Correspondence: aaljanad@auaf.edu.af (A.A.); nadia@uniten.edu.my (N.M.L.T.)

Abstract: Hourly global solar irradiance (GSR) data are required for sizing, planning, and modeling of solar photovoltaic farms. However, operating and controlling such farms exposed to varying environmental conditions, such as fast passing clouds, necessitates GSR data to be available for very short time intervals. Classical backpropagation neural networks do not perform satisfactorily when predicting parameters within short intervals. This paper proposes a hybrid backpropagation neural networks based on particle swarm optimization. The particle swarm algorithm is used as an optimization algorithm within the backpropagation neural networks to optimize the number of hidden layers and neurons used and its learning rate. The proposed model can be used as a reliable model in predicting changes in the solar irradiance during short time interval in tropical regions such as Malaysia and other regions. Actual global solar irradiance data of 5-s and 1-min intervals, recorded by weather stations, are applied to train and test the proposed algorithm. Moreover, to ensure the adaptability and robustness of the proposed technique, two different cases are evaluated using 1-day and 3-days profiles, for two different time intervals of 1-min and 5-s each. A set of statistical error indices have been introduced to evaluate the performance of the proposed algorithm. From the results obtained, the 3-days profile's performance evaluation of the BPNN-PSO are 1.7078 of RMSE, 0.7537 of MAE, 0.0292 of MSE, and 31.4348 of MAPE (%), at 5-s time interval, where the obtained results of 1-min interval are 0.6566 of RMSE, 0.2754 of MAE, 0.0043 of MSE, and 1.4732 of MAPE (%). The results revealed that proposed model outperformed the standalone backpropagation neural networks method in predicting global solar irradiance values for extremely short-time intervals. In addition to that, the proposed model exhibited high level of predictability compared to other existing models.

Keywords: solar irradiance; short time interval; hybrid AI prediction models; short-term solar irradiance prediction; energy management

Citation: Aljanad, A.; Tan, N.M.L.; Agelidis, V.G.; Shareef, H. Neural Network Approach for Global Solar Irradiance Prediction at Extremely Short-Time-Intervals Using Particle Swarm Optimization Algorithm. *Energies* **2021**, *14*, 1213. https://doi.org/10.3390/en14041213

Academic Editor: Jesús Polo

Received: 24 December 2020
Accepted: 22 January 2021
Published: 23 February 2021

1. Introduction

Sustainable energy sources such as photovoltaics (PV) generation is becoming increasingly important in the current times due to the depletion of natural resources, increasing energy demand, high cost of new fossil-fuel generation and transmission power system infrastructure, and worsening greenhouse gas effects. However, PV output power is not dispatchable in terms of supply and demand because of inherent intermittency in solar irradiance. Be it large-scale or nanogrid PV generation, energy storage devices such as batteries and ultracapacitors are required to manage energy and transient power demand,

respectively [1]. Therefore, prediction of solar irradiance is essential in order to correctly size a solar PV power plant and energy storage system and to optimize the corresponding energy management system.

There are many predictive and artificial intelligence (AI) techniques that are proposed to predict solar irradiance and eliminate the limitations of measuring instrument, which feature high efficiency, flexibility, consistency, reliability, and so on. To obtain GSR data, different models are proposed by researchers, such as empirical [2], physical [3], and machine learning [4] models. Among them, machine learning models, presenting high accuracy and wider applicability, are widely studied worldwide [5]. Most of the prediction of GSR using the two methods have been for daily, hourly, or half-hourly time intervals. There has been no extensive studies on short-time, few minutes or few seconds, interval GSR prediction, which is advantageous for real-time compensation by energy management system (EMS) of PV generation and with battery or ultracapacitor.

In classical modelling methods, GSR are structured as standalone models. Artificial neural network is one of the more common AI technique that is used for prediction of GSR [6–8]. They include a variety of models such as multilayer perception neural networks (MLP-NNs) [9], radial basis function neural networks (RBF-NNs) [10], generalized regression neural networks (GR-NNs) [11], extreme learning machines [12], deep learning neural networks [13], convolutional neural networks [14], and so on. For example, authors of [15] compared MLP-NNs, RBF-NNs, and GR-NNs for daily global solar radiation estimation in three climate zones of China, illustrating that MLP-NNs and RBF-NNs performed much better than GR-NNs. Authors of [16] used latitude, longitude, and altitude geographical parameters and meteorological parameters like relative humidity, air pressure, clearness index (Kt), and average temperature (Ta) as inputs of ANN models to predict the GSR of stations in Zimbabwe. The results showed that Kt is the most effective feature to predict the GSR. Authors of [17] evaluated the performance of GSR prediction over other ANN techniques and architectures such as multilayer perceptron neural network, a neural network using wavelet transform, Elman Neural Network, and radial basis neural network. The performance of GSR prediction using other AI techniques such as support vector machine (SVM) [18], adaptive neuro-fuzzy inference system (ANFIS) [19], kernel-based nonlinear extension of Arps decline model and gradient boosting with categorical features support [20], and support vector regression [21] have also been investigated. Empirical methods are also widely discussed and evaluated as a predictive model of GSR in many countries [22]. Authors of [23], developed an empirical model for GSR in southwest Turkey where two models, cubic and quadratic are found to be the appropriate models. The drawbacks and limitations of these standalone and classical models are the insufficient capacity to capture and ascertain the deterministic features of meteorological data. The utilization of the temperature as a crucial input key features in ANN model is suggested by some researchers to have a high predictive performance [24].

Hybrid models are implemented as data-driven models to enhance and increase the capability of GSR prediction. Ibrahim and Tamer proposed a hybrid RF technique-based firefly algorithm (FFA) for predicting hourly GSR [25]. FFA is used to optimize the number of trees and leaves of a random forest (RF) technique. The RF technique is compared with different standalone and hybrid prediction models like ANN and ANN based FFA, respectively. The Mycielski-Makrov hybrid model is proposed to predict solar irradiance by using historical solar irradiance data without needing any other parameters [26]. The results of the model achieved better accuracy when it is compared with standalone Mycielski model. In [27], the solar irradiance performance and efficiency of hybrid model using auto-regressive average moving (ARMA) and feed-forward time-delay neural network showed improvement in prediction accuracy compared with classical ARMA model. In a similar manner, a number of independent hybrid day-of-the-year based models such as ANFIS with chaotic firefly algorithm and ANFIS with whale optimization algorithm with simulated annealing and roulette wheel selection have been employed in estimating GSR in China, where the variability of climate is wide-ranging [28]. The hybrid methods would

increase the estimation accuracy of GSR despite the wide-ranging climate variability. Improvement in GSR prediction is also performed by hybridizing extreme-learning-machine and neural-grouping genetic algorithms into a single model, where optimal feature selection is achieved [29].

This study aims to overcome the drawback of standalone AI models by examining the adaptability, efficiency and accuracy of the hybrid backpropagation neural network and particle swarm optimization (BPNN-PSO) method for prediction of solar irradiance in very short-time intervals and fast changing climate conditions as there has been no extensive studies on prediction of GSR in those conditions in a tropical country. This paper also designs and develops a high-efficiency prediction model through the use of the actual meteorological data from Kajang, Malaysia. The meteorological data include pressure, humidity, temperature, wind speed, wind direction, and diffuse and direct irradiances.

The proposed PSO is used inside the BPNN to improve the prediction performance by reducing the error with actual data and improving the convergence rate by minimizing the objective function. The PSO optimizes hidden layers, neurons, and learning rate of BPNN architecture. The best minimized combination value of these three parameters in BPNN is the main objective function. The accuracy of the developed hybrid BPNN-PSO model is compared and evaluated with other existing model using reliable statistical indicators, such as root mean square error (RMSE), mean squared error (MSE), mean absolute error (MAE), and mean absolute percentage error (MAPE).

This paper is organized as follows: first, a literature review is presented. In Section 2, the BPNN algorithm is presented. In Section 3, data preparation for training and testing the PSO algorithm working concepts, and the performance evaluation of the model is discussed. In Section 4, the simulations results are analyzed. Finally, the achievements of the proposed method are highlighted in the conclusion.

2. Theory of Backpropagation Neural Network Structure

The ANN models nonlinear systems and make every effort to create the function of the human brain in a simulation environment through distributed processing. The ANN consists of neurons, which are simple connected elements that have the advantage in solving complex nonlinear relationship between system input and output [30,31].

Figure 1 shows the structure of the BPNN model employed. The model consists of seven meteorological inputs that are obtained from Kajang, Malaysia, which include pressure (P), temperature (T), humidity (H), wind speed (WS), wind direction (WD), irradiance direct (IDR), and irradiance diffuse (IDF), a few hidden layers and one GSR as output parameter. In order to predict GSR, this paper employs the Levenberg-Marquardt backpropagation algorithm to train the multi-layer perceptron of the ANN model in Matlab. The Levenberg-Marquardt algorithm has been selected due to its minimal localization error as well as its efficiency and speed [32]. The training of ANN using Levenberg-Marquardt back propagation algorithm involves three phases: (a) The feedforward phase, (b) the computation and backpropagation of the associated error, and (c) the adjustment of the weights. All inputs and outputs of the BPNN are expressed by the following equations:

$$Input = \begin{bmatrix} T_1 & H_1 & P_1 & WS_1 & WD_1 & IDR_1 & IDF_1 \\ T_2 & H_2 & P_2 & WS_2 & WD_2 & IDR_2 & IDF_2 \\ \vdots & \vdots & \vdots & \vdots & \vdots & \vdots & \vdots \\ T_n & T_n & P_n & WS_n & WD_n & IDR_n & IDF_n \end{bmatrix} \quad (1)$$

$$Output = \begin{bmatrix} GSR_1 \\ GSR_2 \\ \vdots \\ GSR_n \end{bmatrix} \quad (2)$$

where GSR is the global solar irradiance of the meteorological datasets.

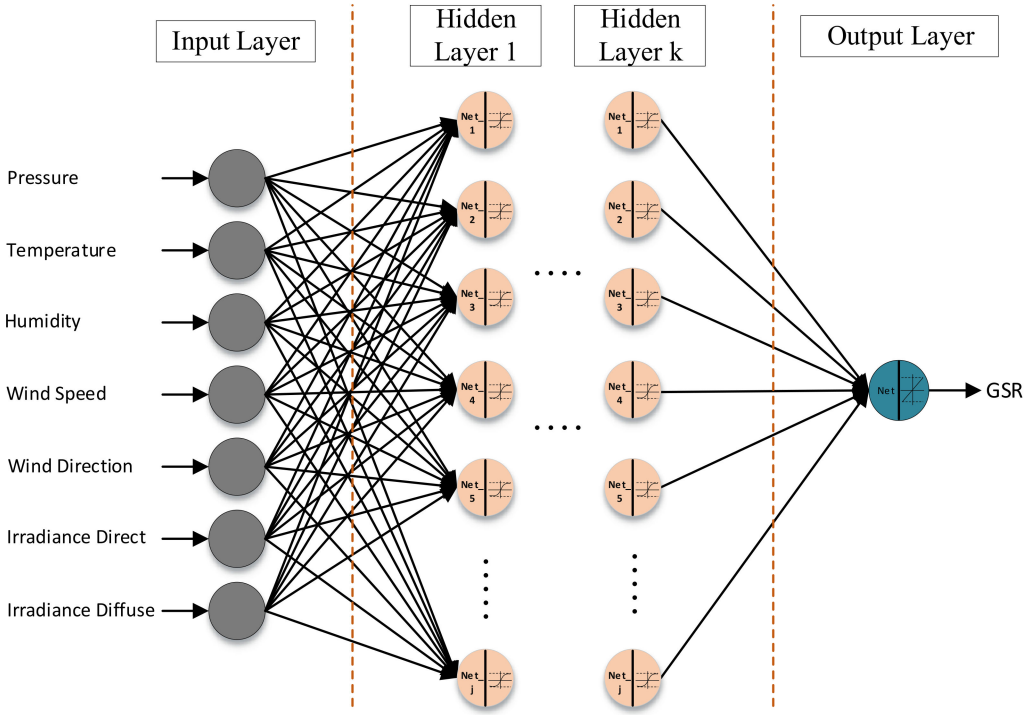

Figure 1. Backpropagation neural networks (BPNN) structure with seven inputs, one output, and multi hidden nodes.

During the feed-forward phase of ANN training, data samples consisting of seven input values (*P*, *T*, *H*, *WS*, *WD*, *IDR*, and *IDF*) and one output or target value *GSR* are presented into the ANN. The explanation of BPNN working progress is summarized in the following steps:

Step 1: The weight and bias are randomly initialized.

Step 2: The input layer relays the input signals to the hidden nodes. Then, the variables in the hidden nodes are calculated by using [33],

$$net = Z_{in\_j} = Pw_{1j} + Tw_{1j} + Hw_{1j} + WSw_{1j} + WDw_{1j} + IDRw_{1j} + IDFw_{1j} \quad (3)$$

where Z_{in} the input of the hidden nodes, and j is the number of hidden nodes that is calculated by using the PSO and w is the weight factor.

Step 3: The hidden layer is calculated by using the sigmoid function and it is given by,

$$Z(net) = \frac{2}{1 + e^{-net}} - 1 \quad (4)$$

For input pattern p, the i-th input layer node holds xp,i. Net input to j-th node in the hidden layer is,

$$net_j = \sum_{i=0}^{n} \left(w_{j,i} x_{p,i} + \theta_{j,i} \right) \quad (5)$$

where, $w_{j,i}$ is the weight from the input layer to the hidden layer, $\theta_{j,i}$ represents the bias from the input layer to the hidden layer. Output of j-th node in the hidden layer is,

$$x_{p,j} = Z_j \left(\sum_{i=0}^{n} \left(w_{j,i} x_{p,i} + \theta_{j,i} \right) \right) \quad (6)$$

Net input to k-th node in the output layer is,

$$net_k = \sum_{j} \left(w_{k,j} x_{p,k} + \theta_{k,j} \right) \quad (7)$$

where, $w_{k,i}$, $\theta_{k,j}$, are the weight and bias from the hidden layer to the output layer, respectively. Output of k-th node in the output layer is,

$$O_{p,k} = Z_k\left(\sum_j\left(w_{k,j}x_{p,k} + \theta_{k,j}\right)\right) \tag{8}$$

Step 4: In the BPNN training, after executing the feed-forward phase, the next phases are to compute the backpropagation of the associated error and then adjust the weights. During training, the *GSR* is compared with its target value in the sample data to determine the associated error (e). Based on this error, factor δ_k that is used to distribute the error at the output layer back to all hidden nodes is given by,

$$\delta_k = Z_k(1 - Z_k)(T_k - Z_k) \tag{9}$$

where T_k is the true output (GSR). The error in the hidden layer is calculated as

$$\delta_j = Z_j(1 - Z_j)\delta_k w_{k,j} \tag{10}$$

Step 5: BPNN in this phase, updates error and biases. Weights are updated using the following equations

$$\Delta w_{k,j} = \alpha\delta_k S_j \tag{11}$$

$$w_{k,j} = w_{k,i} + \Delta w_{k,j} \tag{12}$$

$$\Delta w_{j,i} = \alpha\delta_k x_p \tag{13}$$

$$w_{j,i} = w_{j,i} + \Delta w_{j,i} \tag{14}$$

where α is the learning rate which can be assigned values between 0 and 1.

Biases are updated using the following equations

$$\Delta\theta_{k,j} = \alpha\delta_k \tag{15}$$

$$\theta_{k,j} = \theta_{k,j} + \Delta\theta_{k,j} \tag{16}$$

$$\Delta\theta_{j,i} = \alpha\delta_j \tag{17}$$

$$\theta_{j,i} = \theta_{j,i} + \Delta\theta_{j,i} \tag{18}$$

The adjustment of the weights from the input to the hidden layer is based on factor δ_j in (10) and the activation of the input features. Using (4) to (18), the BPNN process is repeated for all the data set samples to achieve one epoch. The training process will continue until the error goal or the predefined epoch is achieved. After the training process, the ANN can be utilized to generate the reference GSR with new input data.

3. Methodology Proposed Hybrid BPNN-PSO for Predicting GSR

The BPNN architecture is implemented at the process of training the GSR due to its capability to minimize output error by optimizing the input weight values of the output layer. However, three significant parameters in BPNN architecture namely hidden layers (HL), number of neurons (Ne), and learning rate (LR) are normally set based on trial and error method, which is time consuming. In order to further enhance the performance of the GSR prediction and overcome the time-consuming process of trial and error method, the PSO algorithm is utilized to find the optimal best combination of the dimension array. In addition, PSO is used to give reliable GSR prediction with less variance, less error, and the best fitting for the prediction function. Figure 2 shows the schematic diagram for prediction GSR using BPNN based PSO. The process is categorized into three phases which are clearly illustrated as follows:

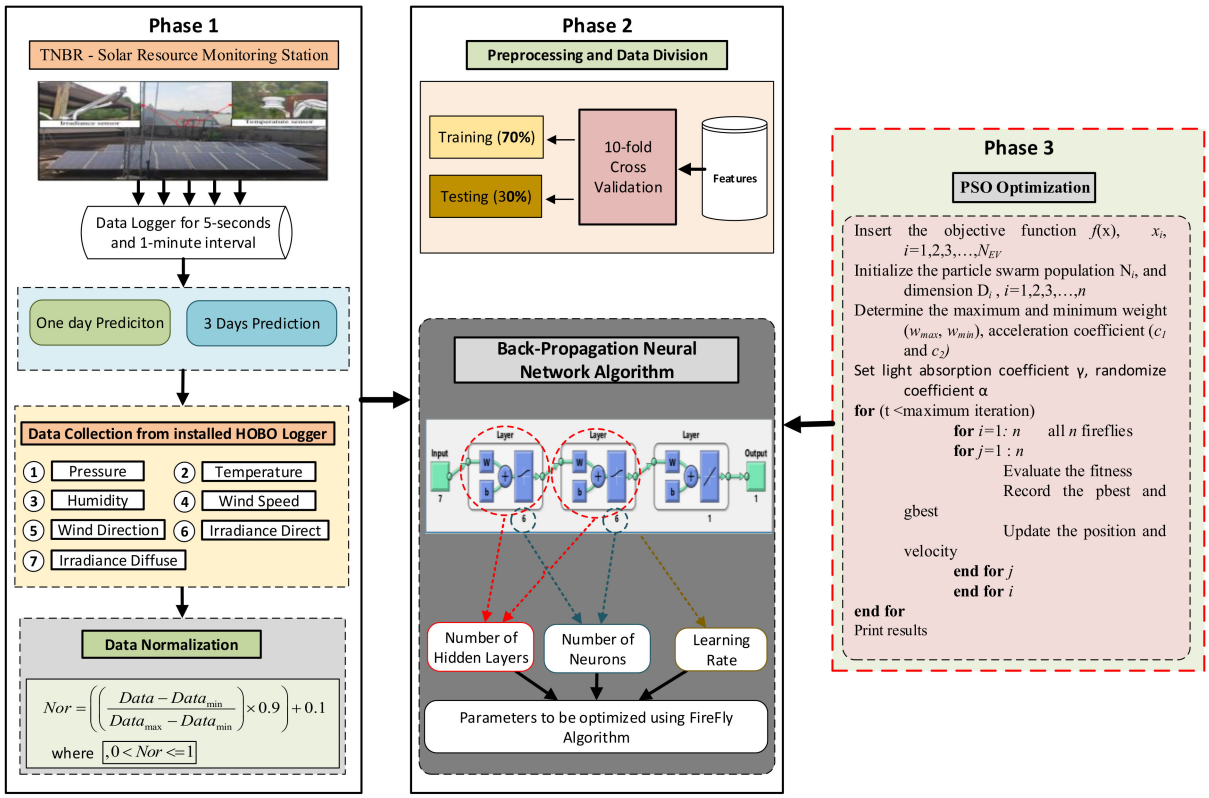

Figure 2. The structure of the proposed backpropagation neural network based on Particle Swarm Optimization Algorithm (PSO) algorithm.

Phase I: This phase begins with the collection of seven input variables at 5-s and 1-min time intervals. This study has included two profiles for the reason of improving the prediction performance by capturing the nonlinear association of patterns between different meteorological parameters, such as temperature, pressure, humidity, wind speed, wind direction, irradiance direct, and irradiance diffuse. After that, the sample data is moved through the normalization method.

Phase II and III: In these phases, 10-fold cross validation method is used for data pre-processing and division into training and testing observations. Then, the BPNN model is used for GSR prediction where the optimal number of hidden layer neurons and learning rate of BPNN model are computed based on PSO algorithm to enhance the accuracy of GSR.

3.1. Particle Swarm Optimization Algorithm

PSO is a heuristic optimization technique, which is based on population inspired by bird flocking and fish schooling for solving nonlinear problems with both discrete and continuous variables. The PSO algorithm is robust and easy to implement with global exploration capability in various applications [34]. In PSO, the potential solution to the problem being considered is randomly generated though a population individual particles also known as "swarm". Each particle will move at arbitrary velocity across a dimensional search space to find two locations. The swarm will keep two locations. The first location is the best position in the current iteration also known as the local best, and the second location is the best point found in all previous iterations also known as the global best. The velocity and position factors are updated as [35]:

$$V_i^d(t+1) = wV_i^d(t) + c_1 r_1 \left(P_i^d(t) - X_i^d(t) \right) + c_2 r_2 \left(P_t^d(t) - X_i^d(t) \right) \quad (19)$$

$$X_i^d(t+1) = X_i^d(t) + V_i^d(t+1) \quad (20)$$

where c_1 is the social rate, and c_2 is the cognitive rate. r_1 and r_2 denote the randomness in the interval (0,1), V is the velocity factor of agent i at iteration d, t is the present iteration, w is the inertia factor, and X is the position factor.

3.2. Performance Evaluation

To investigate the performance and validate the accuracy of each model, four statistical index errors are implemented. In addition, a previous benchmark study at different sites are compared with the proposed hybrid model. There are various statistical indices that have been used by other researchers [36]. However, MSE, MAE, and MAPE are the most common statistical error indexes [37]. Therefore, in this study, the performance evolution of the proposed techniques are investigated through the following indexes:

$$MAE = \sum_{i=1}^{n} \frac{1}{n} x \left| GSR_{A_i} - GSR_{P_i} \right| \text{ W m}^{-2} \quad (21)$$

$$RMSE = \sqrt{\frac{1}{n} \sum_{i=1}^{n} \left(GSR_{A_i} - GSR_{P_i} \right)^2} \text{ W m}^{-2} \quad (22)$$

$$MSE = \frac{1}{n} \sum_{i=1}^{n} \left(GSR_{A_i} - GSR_{P_i} \right)^2 \left(\text{W m}^{-2} \right)^2 \quad (23)$$

$$MAPE = \frac{1}{n} \sum_{i=1}^{n} \left| \frac{GSR_{A_i} - GSR_{P_i}}{GSR_{P_i}} \right| \% \quad (24)$$

where error = $GSR_{A_i} - GSR_{P_i}$, GSR_{A_i} is the state of charge of the actual data, and GSR_{P_i} is the state of charge of the predicted data, and n is the number of samples.

3.3. Data Preparation and Model Execution

The prediction of the GSR for one-day and three-day profiles begins with the collection of seven input variables at 5-s and 1-min time intervals. This study has included two profiles for the reason of improving the prediction performance by capturing the nonlinear association of patterns between different meteorological parameters, such as temperature, pressure, humidity, wind speed, wind direction, irradiance direct, and irradiance diffuse. At the first stage, the data have been collected from the TNBR—Solar Resource Monitoring Station, located in Kajang, Malaysia, with different time intervals. The data is collected from 1 March 2013 to 15 February 2014 using a high sampling data logger at a sampling rate of 5 and 30 s for 1, 5, 30, and 60 min interval. This measurement was taken as part of a Seeding Fund Project TNBR/SF140/2010 entitled "Development of Solar Research Facility for studies of Grid Connection of Utility Scale Solar Power Plant". The Solar Resource Measurement was performed as follow: (a) GSR was measured by a CMP11 pyranometer, (b) Diffuse irradiance was measured by a CMP11 pyranometer and shaded by a shading ball attached, and (c) Direct irradiance was measured by a CHP1 pyrheliometer. The irradiance and temperature were measured using a solar pyranometer sensor and a temperature sensor, respectively. All measurements were performed instantaneously for every 5-s and 1-min time intervals and the measurements were recorded using the DT80 data logger.

The available meteorological data features would guarantee a high efficiency prediction of the solar irradiance during the short time intervals (5-s and 1-min) without any new features. Moreover, to increase and improve the accuracy of the output GSR parameter, all other possible data features that may have a direct effect on the output parameter performance are included in the predictive models. All the saved input datasets are normalized before being trained by BPNN model to increase the robustness and efficiency of the system.

Besides, it enhances the convergence rate of the predicted GSR. In this study, the data normalization range is from 0 to 1 and is determined as:

$$Norm = \left(\left(\frac{Data - Data_{\min}}{Data_{\max} - Data_{\min}} \right) \times 0.9 \right) + 0.1 \quad (25)$$

where the $Data_{\max}$ and $Data_{\min}$ are the maximum and minimum value of the BPNN trained dataset. The testing dataset is also normalized with the same range limit. The trained dataset has been divided to 70% for training and 30% for testing, where 10-fold cross validation method is implemented in all input arrays.

Figure 3 shows the flowchart of the proposed hybrid BPNN-PSO implementation for predicting the PV GSR in detail. The implementation procedure of the proposed hybrid technique in determining the optimum number of hidden neurons (Ne), hidden layers (HL), and learning rate (LR).

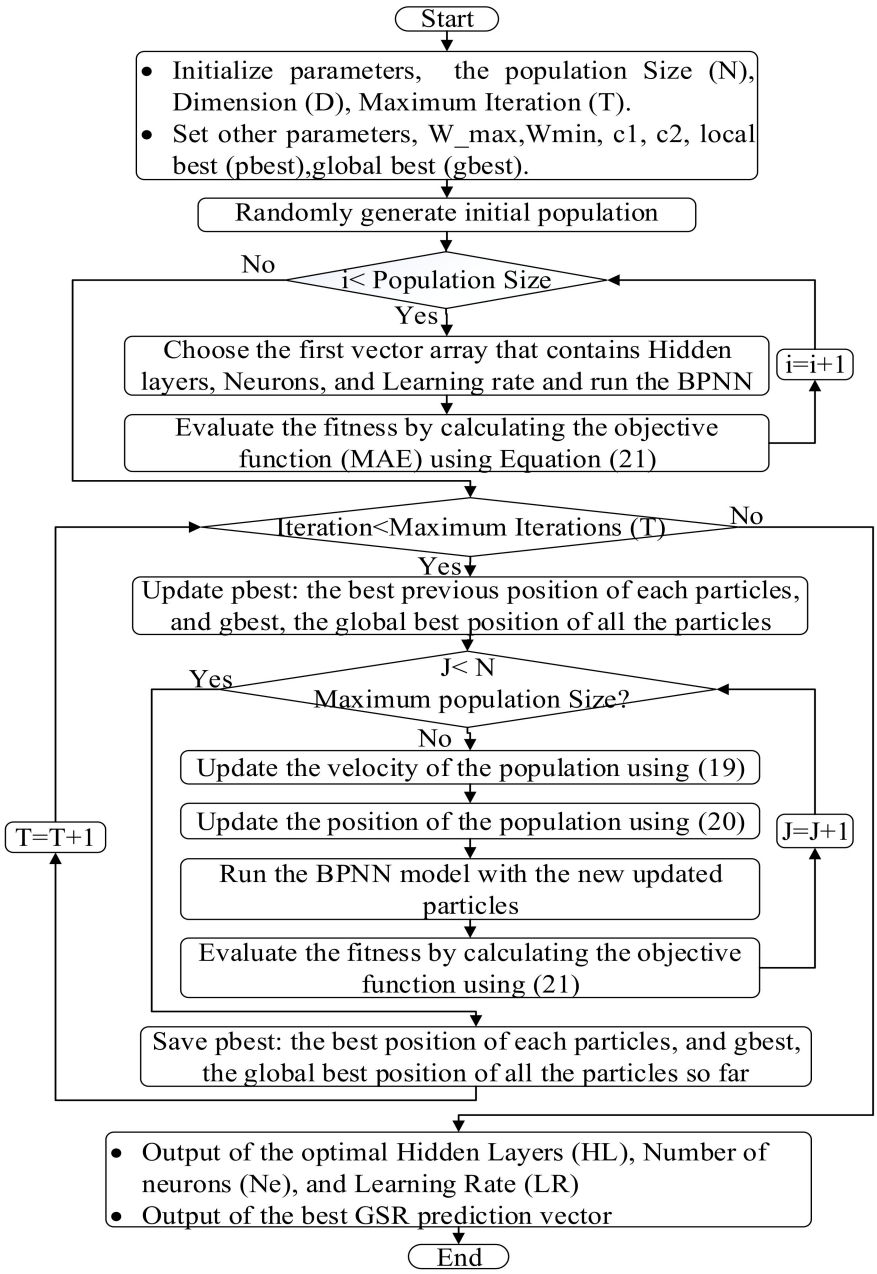

Figure 3. Flowchart of the proposed hybrid backpropagation neural network based on particle swarm optimization algorithm (BPNN-PSO) model.

Table 1 presents the parameters used in the initialization of the algorithm. Then the initial local and global best positions, P_{best} and G_{best} are randomly generated. In order to train the ANN and evaluate the fitness value, the number of learning rate, hidden neurons, and layers should be selected. The objective function MAE is evaluated based on (21) and the new P_{best} and G_{best} are updated. The velocity and position are computed and updated using (19) and (20). If the position is rejected, other combinations have to be identified. Training of ANN and evaluation of MAE should be repeated until the maximum population size is reached or when P_{best} is lower than G_{best}. If the local best value is less than global best value, the previous is updated as the global best value. The process is iterated until the stop criterion is reached so as to obtain the optimal hidden layers and hidden neurons.

Table 1. PSO algorithm initialization parameters.

Parameters	Symbol	Value
Population Size	N	10
No. of Dimensions	D	5
No. of Iterations	T	500
Maximum Weight	W_{max}	0.9
Minimum Weight	W_{min}	0.4
Acceleration Coefficient	c_1, c_2	2

4. Discussion and Results

4.1. Objective Function Performance of PV Solar Irradiance

Figures 4 and 5 depict solar irradiance convergence results using BPNN with the assistance of PSO algorithm, which are evaluated under different time intervals of 5-s and 1-min for both 1-day and 3-days profiles. The performance evaluation is represented by statistical index error or objective function (MAE), which compares the simulation convergence results over 100 iterations. The optimization parameters of population size and the iteration numbers are standardized with 4 and 100 maximum iterations, respectively. In Figure 4, the proposed hybrid algorithm BPNN-PSO shows less error compared to actual GSR data, where the minimum objective function MAE values obtained from 3-Days profile for 5-s and 1-min time intervals are 0.7537, and 0.2754, respectively. Figure 5 presents the one-day profile with better convergence rate over the 3-days profile for both time intervals of 5-s and 1-min with 0.1000 and 0.0956, respectively.

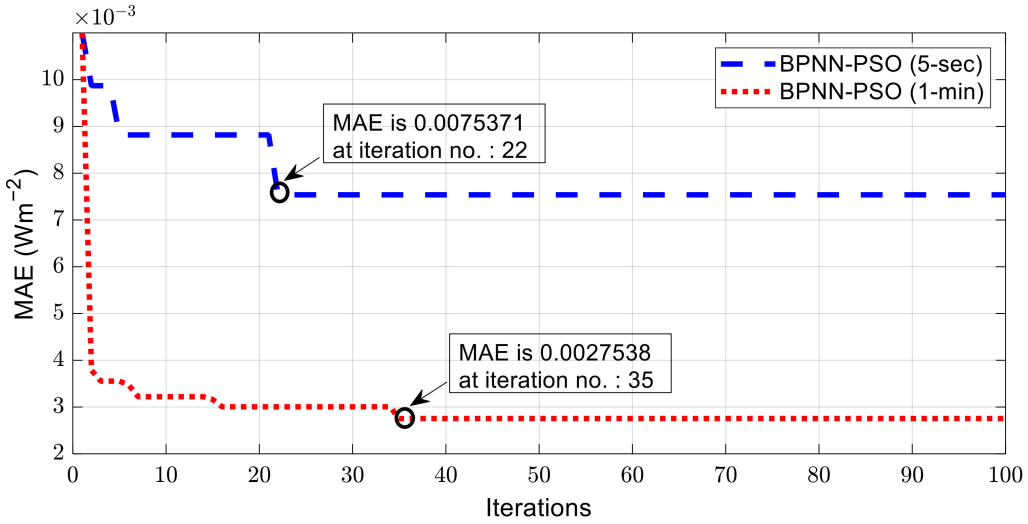

Figure 4. The convergence performance curves of solar irradiance prediction for 3-days, with 1-min and 5-s time interval.

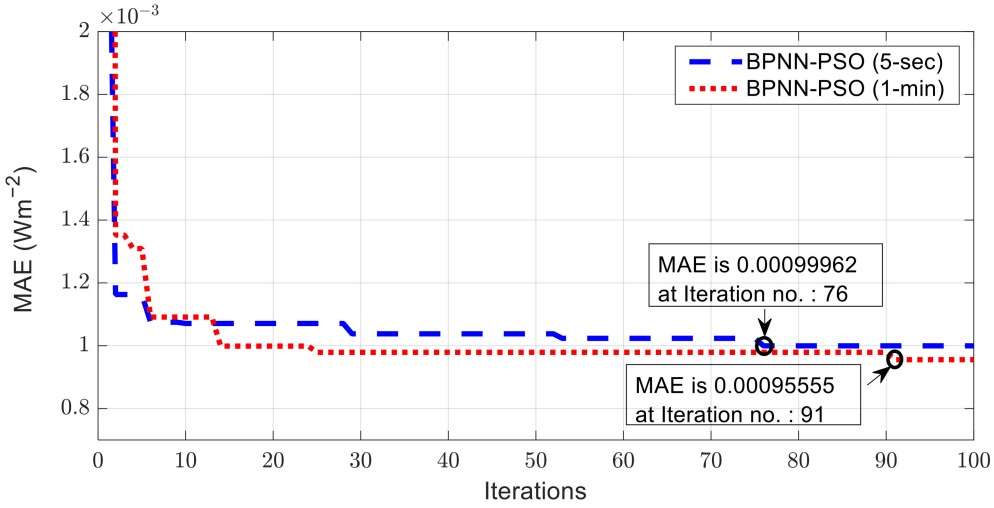

Figure 5. The convergence performance curves of solar irradiance prediction for 1-Day, with 1-min and 5-s time interval.

Other statistical index errors like MSE, RMSE, and MAPE are used to give more extensive analysis of the output performance for both profiles in 1 day and 3 days as shown in Table 2. Under the nonlinearity behaviors of GSR, the proposed predictive hybrid technique is investigated with the aforementioned analytical index error tools, where all other statistical index errors like RMSE, MSE, and MAPE, show the superiority of the proposed BPNN-PSO technique in 3-days profile with 1.7078, 0.0292, and 31.4348 for 5-s, and 0.6566, 0.0043, and 1.4732 for 1-min time intervals, respectively. Likewise, the 1-day profile shows the superior performance of the proposed hybrid model with 0.1911 (RMSE), 0.0004 (MSE), and 0.7484 (MAPE) for 5-s, and 0.2032, 0.0004, and 1.1271 for 1-min time intervals.

Table 2. Performance comparison using statistical index errors of the 1-day and 3-days profiles.

Type of Profile	Time Intervals	RMSE × 10^{-2} (W m^{-2})	MAE × 10^{-2} (W m^{-2})	MSE × 10^{-2}	MAPE [%]
3-Days Profile	5-s	1.7078	0.7537	0.0292	31.4348
	1 min	0.6566	0.2754	0.0043	1.4732
1-Day Profile	5-s	0.1911	0.1000	0.0004	0.7484
	1 min	0.2032	0.0956	0.0004	1.1271

4.2. PV Solar Irradiance Optimal Parameters

The optimal parameters HL, Ne, and LR, acquired after implementing the heuristic optimization algorithms PSO for the 1-day and 3-days profiles are shown in Table 3. In the 3-days profile, the BPNN-PSO algorithm attains hidden layers of 1 (7 Ne) and 2 (14 and 9 Ne) after 22 and 35 iterations for 5-s and 1-min time intervals. In the 1-day profile, the proposed BPNN-PSO achieved the optimal value of hidden layers of 2 (8 and 2 Ne) and (9 and 11 Ne) after 76 and 91 iterations for 5-s and 1-min time intervals, respectively. In contrast, the best learning rate values of 3-days and 1-day profiles are 0.1295, 0.7373, 0.5946, and 0.6481 during both time intervals of 5-s and 1-min, respectively.

4.3. PV Solar Irradiance Prediction

The input parameters considered during the training process of BPNN and PSO are the seven input as shown in Figure 2. The selection of the input features is set to seven after conducting a set of trial-and-error tests to the predictive models, the increase of the input features from one to seven increases the performance of the proposed predictive model

BPNN-PSO. Any further increase in the number of input features after seven did not show further increase in the performance of the BPNN and PSO.

Table 3. Optimal parameters of 1 and 3-Days profile at 5-s and 1-min time intervals.

Profile	Time Interval	Hidden Layers	Neuron 1	Neuron 2	Neuron 3	Learning Rate	Number of Iterations
3-Days	5-s	1	7	0	0	0.1295	22
	1-min	2	14	9	0	0.7373	35
1-Day	5-s	2	8	2	0	0.5946	76
	1-min	2	9	11	0	0.6481	91

Figures 6 and 7 present the predicted solar irradiance using the proposed hybrid BPNN-PSO algorithm and compare the predicted GSR with the reference or actual data. In the figures, the red line represents the actual global solar irradiance data obtained from Kajang, Malaysia, while the blue line is the solar irradiance prediction of the proposed hybrid BPNN-PSO algorithm. It is clearly observed that the performance of the BPNN-PSO over-classed other techniques in both 3-days and 1-day profiles, In Figures 6a and 7a, the predicted solar irradiance of BPNN-PSO is almost aligned with the actual data in both profiles. The time domain response agrees well with the different statistical index errors in Table 2, which proves the superior performance of the proposed technique over the other conventional test techniques under the two time intervals of 5-s and 1-min, respectively. From Figure 7a, it is also noticeable that the results obtained from the proposed BPNN-PSO technique is robust and able to track the fast variation of the actual environmental data. The absolute error between predicted and actual values of 3-Days profile at 5-s and 1-min intervals is represented with the enlarged visual box to provide more clarity on the GSR prediction results, as depicted in Figures 6b and 7b.

Moreover, the 1-day profile is also tested to investigate the ability and adaptability of predictive models under low data set and fast nonlinear environmental change of the solar irradiance. The 1-day profile are used to train the BPNN-PSO with the meteorological data obtained from Kajang, Malaysia, which were recorded on 22 February 2014. The predicted GSR of the proposed BPNN-PSO technique is compared at 5-s and 1-min time intervals. The BPNN-PSO model has a good alignment with the actual data, as depicted in Figures 8a and 9a. The absolute error between predicted values of GSR using the proposed model with the target test values is presented in both 5-s and 1-min time intervals, respectively, as shown in Figures 8b and 9b. The maximum error is approximately 8%, which is negligible.

4.4. Performance Comparison Using Regression Coefficient

The regression coefficient (R) is used as an indicator of the predictive model's training process performance. The predicted data is displayed in black circle, while the blue line represents the reference value (Actual target). The regression coefficient results are very close to unity, which validates the accuracy of the model. The regression values of 3-Days profile with 5-s and 1-min time interval are 0.99951 and 0.99993, as shown in Figure 10. Moreover, Figure 11 shows that the 1-day profile have regression coefficients of 0.99999 at 5-s and 1-min intervals, respectively.

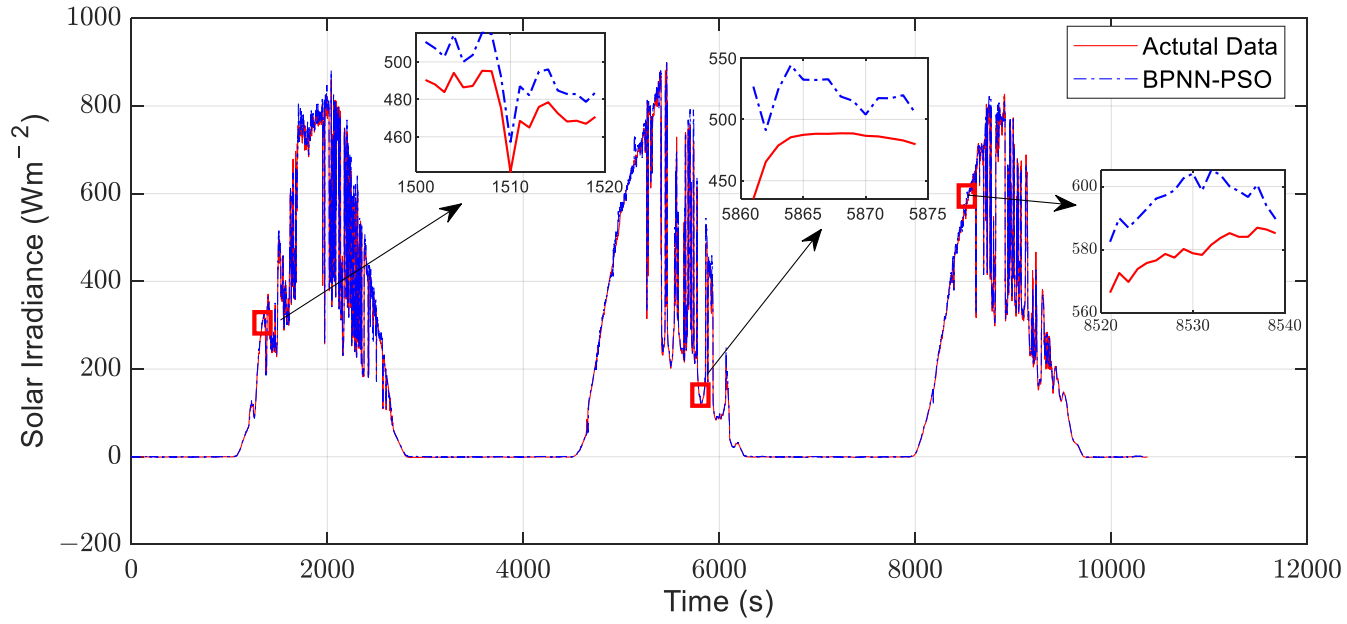

(**a**)

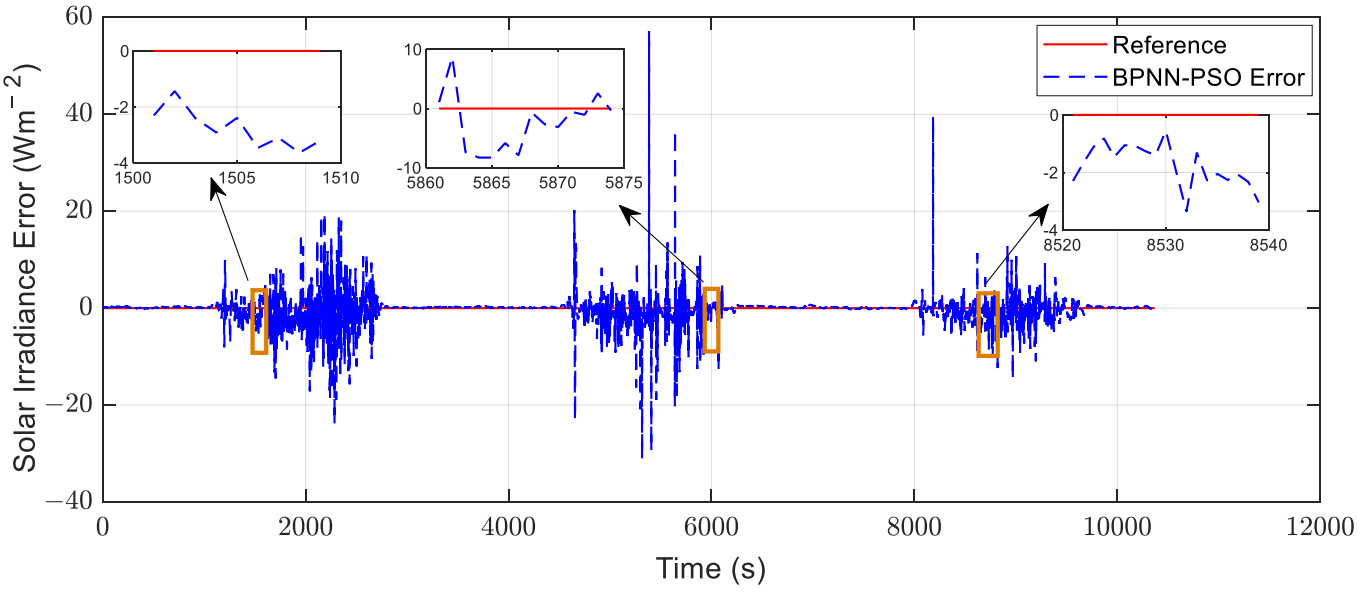

(**b**)

Figure 6. The photovoltaics solar prediction results using 3-days profile with 5-s time interval. (**a**) Solar irradiance prediction. (**b**) Solar irradiance prediction error.

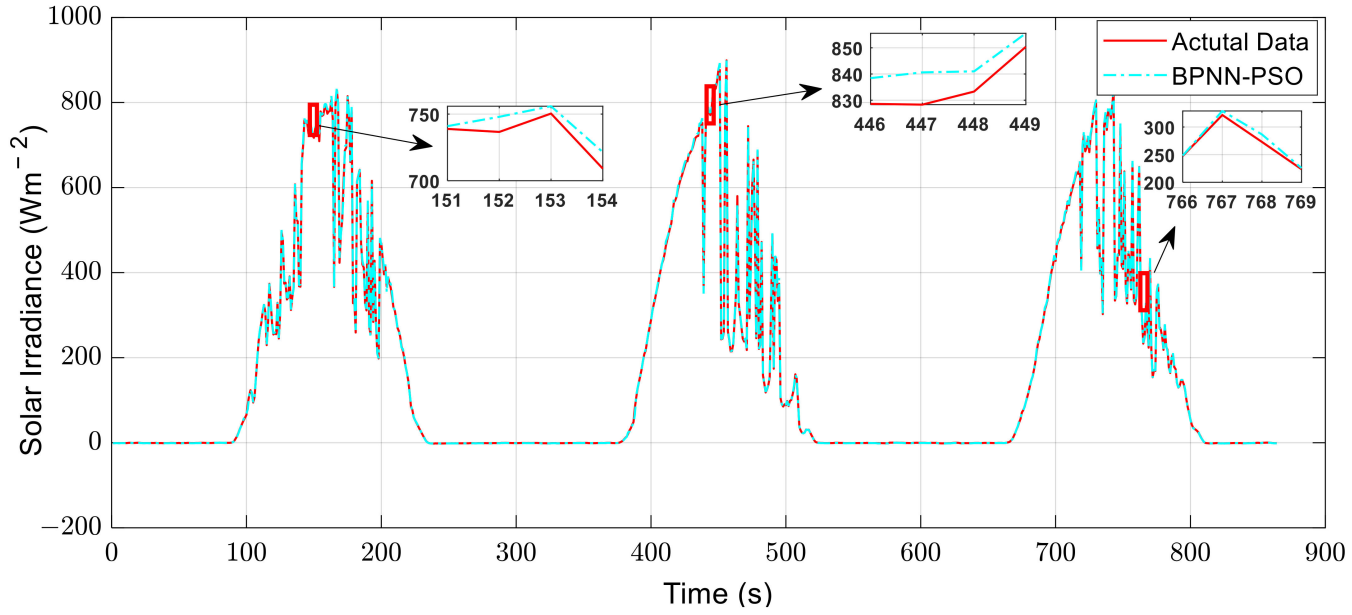

(**a**)

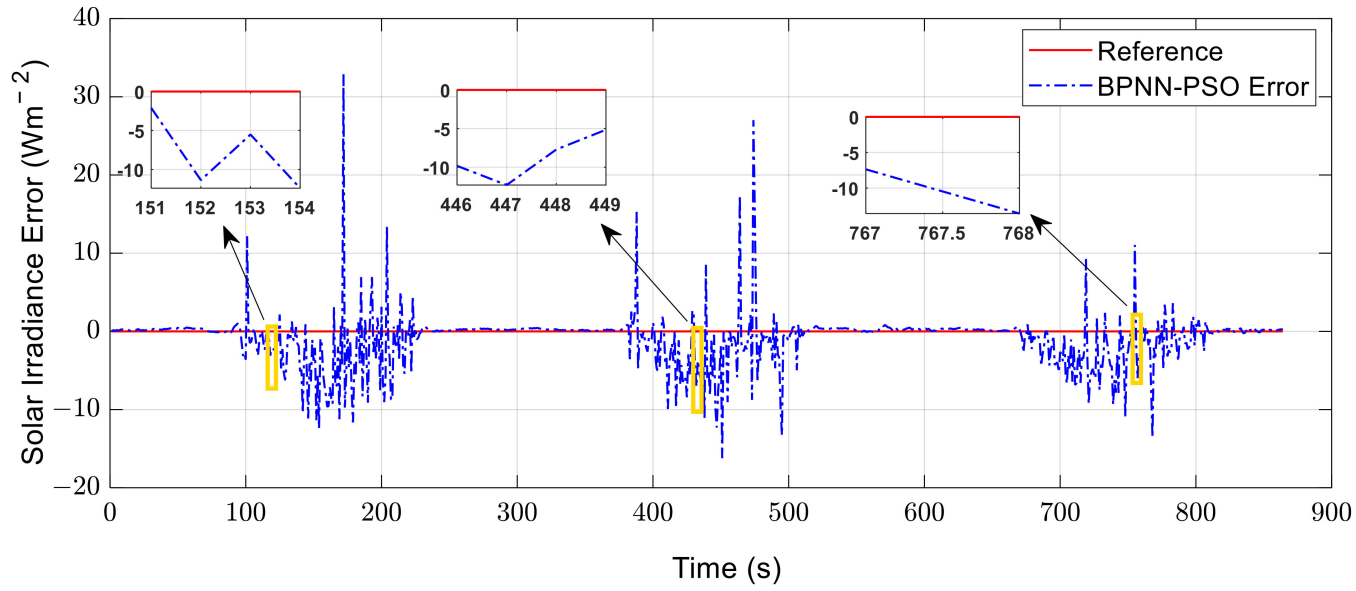

(**b**)

Figure 7. The photovoltaics prediction results using 3-days profile with 1-min time interval. (**a**) Solar irradiance prediction. (**b**) Solar irradiance prediction error.

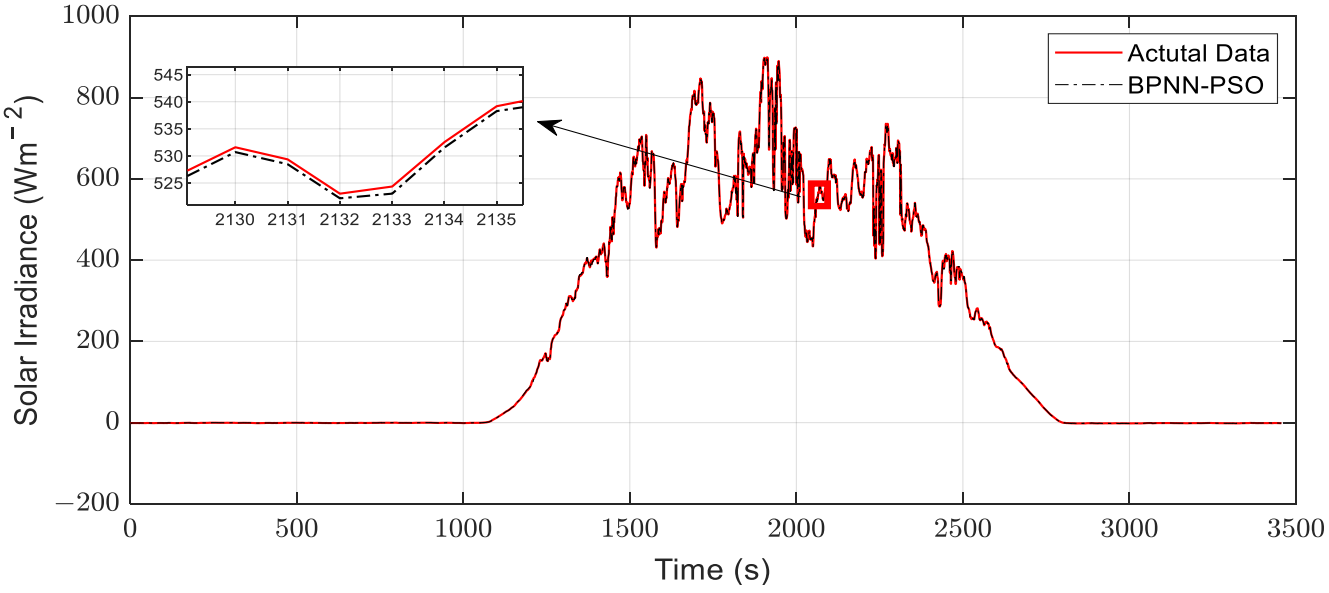

(**a**)

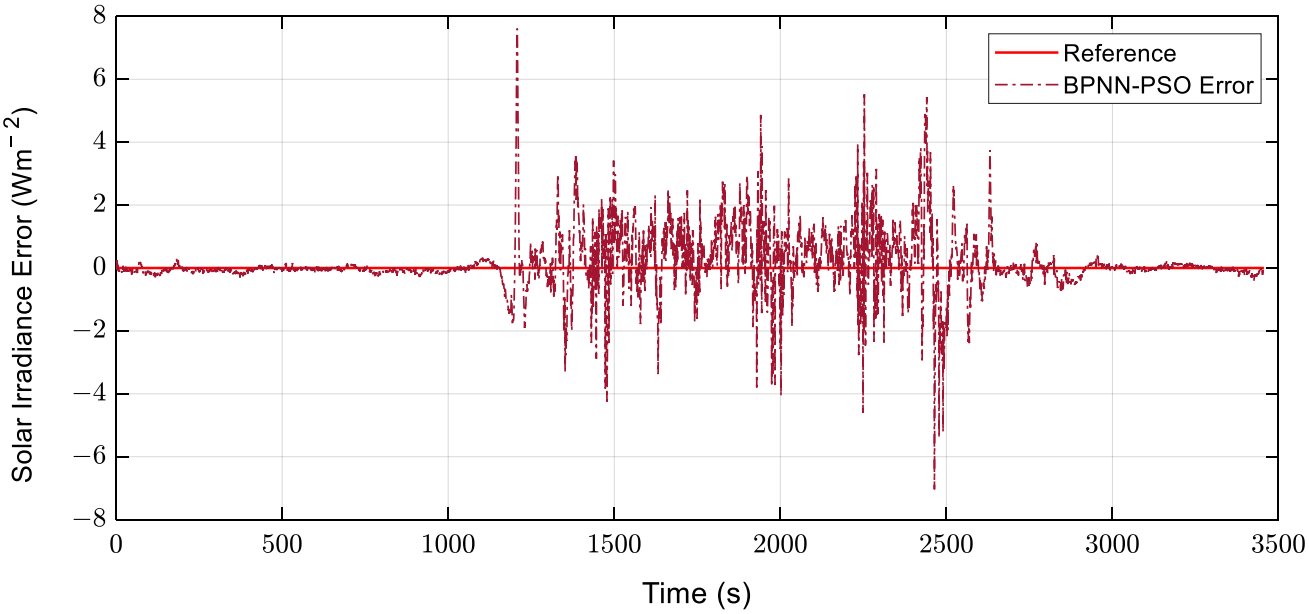

(**b**)

Figure 8. The prediction results using 1-day profile with 5-s time interval. (**a**) Photovoltaics (PV) solar irradiance prediction. (**b**) Photovoltaics (PV) solar irradiance prediction error.

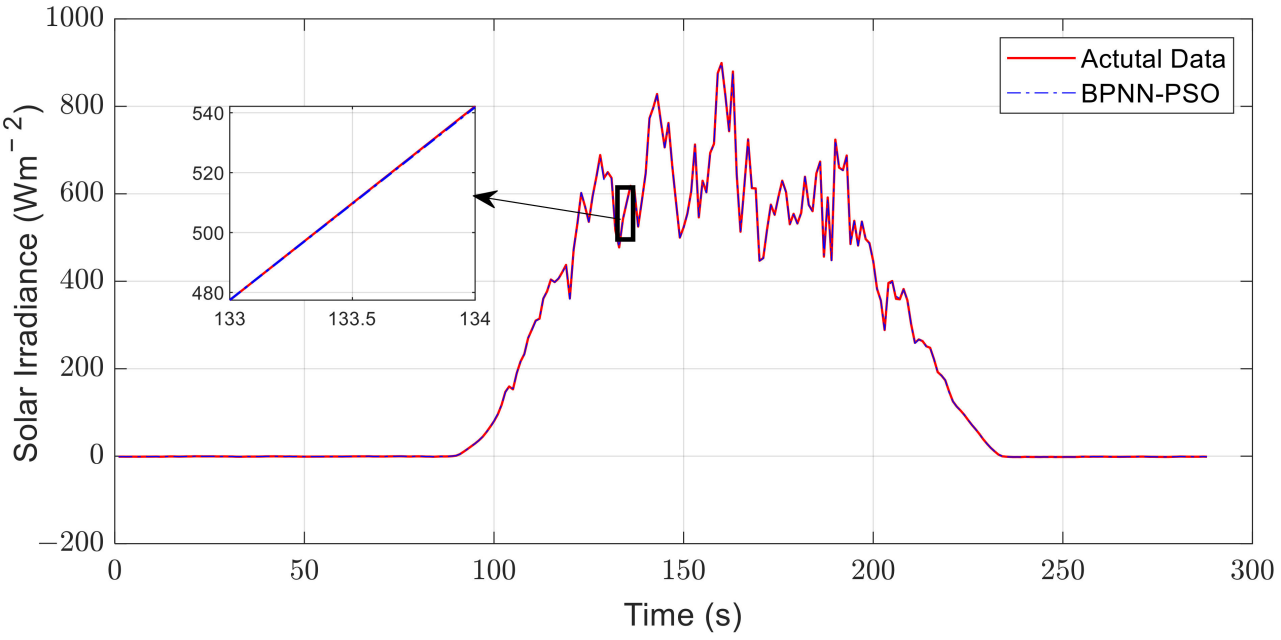

(**a**)

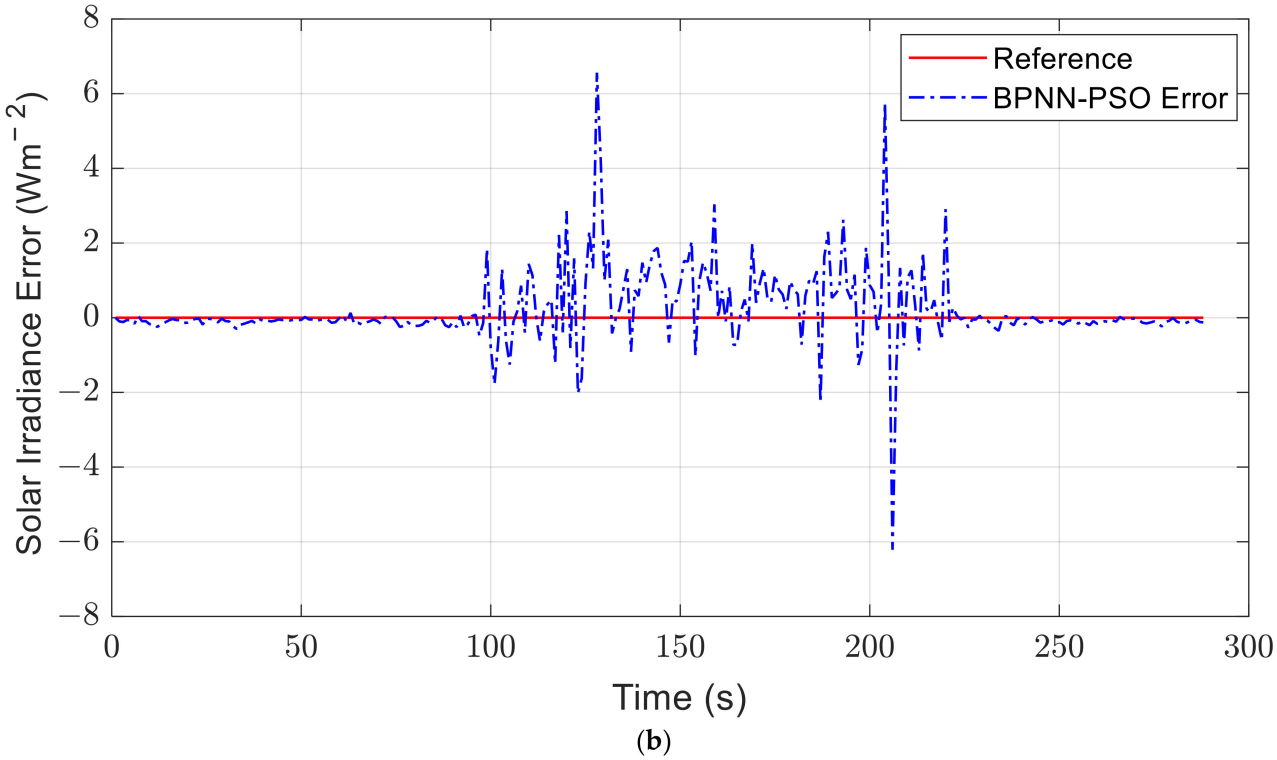

(**b**)

Figure 9. The prediction results using 1-day profile with 1-min time interval. (**a**) Photovoltaics (PV) solar irradiance prediction. (**b**) Photovoltaics (PV) solar irradiance prediction error.

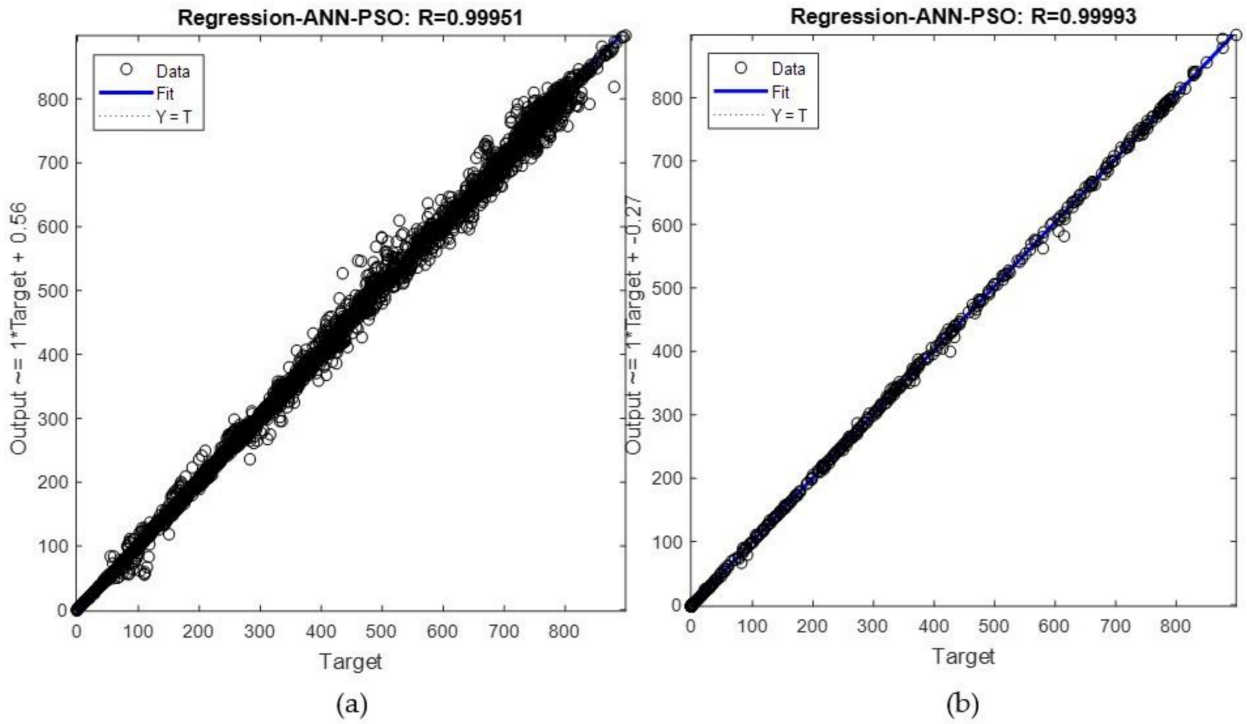

Figure 10. Regression performance of 3-days profile (**a**) BPNN-PSO, with 5-s time interval. (**b**) BPNN-PSO, with 1-min time interval.

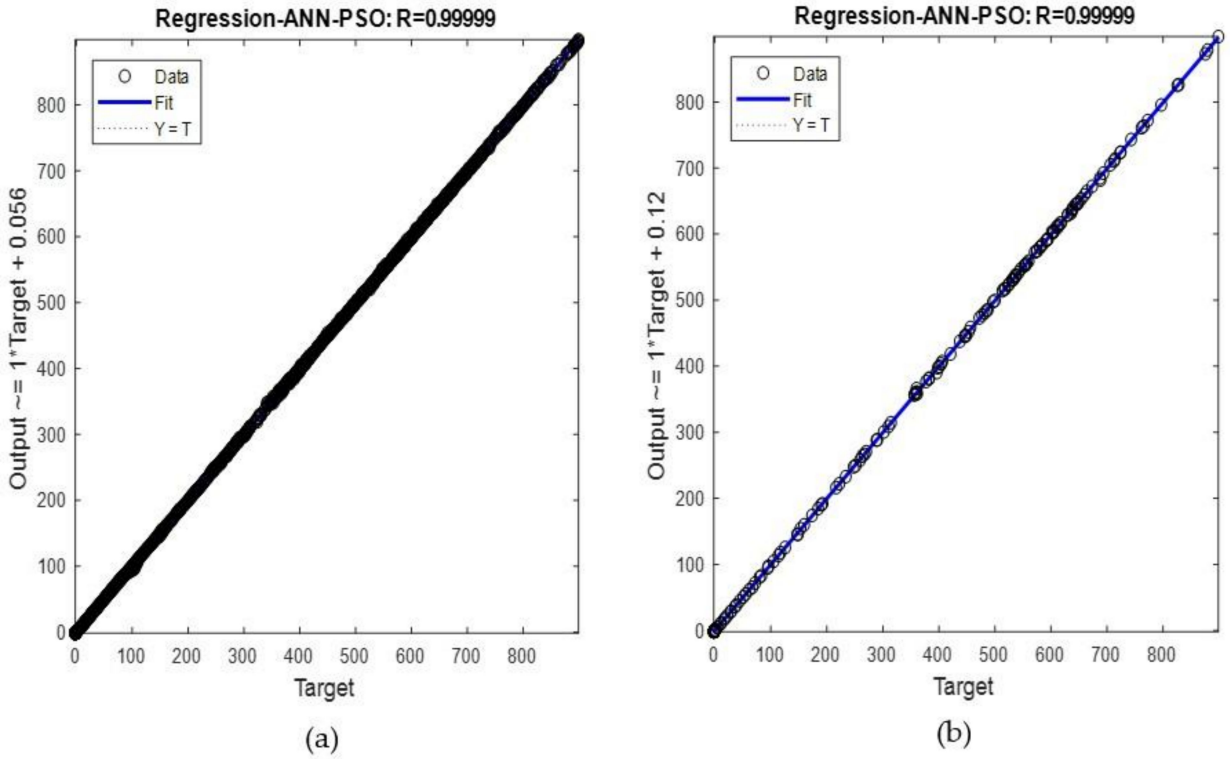

Figure 11. Regression performance of 1-day profile. (**a**) BPNN-PSO with 5-s time interval. (**b**) BPNN-PSO with 1-min time interval.

5. Model Validation with the Existing Methods

Table 4 presents the GSR prediction results of the proposed method that are benchmarked with existing results. The proposed hybrid model is compared with various empirical techniques, artificial intelligence, and hybrid artificial intelligence. The prediction accuracy of the proposed and existing methods is investigated through the four statistical index errors RMSE, MSE, MAE, and MAPE, respectively. The results obtained from the proposed study show greater performance in terms of predictability and improved forecasting capability as compared with the rest of the other methods.

Table 4. Comparison of statistical index errors between proposed method and other existing methods.

Model	Time Interval	Statistical Error Indexes				Study Location
		RMSE ($MJ/m^2/day$)	MAE ($MJ/m^2/day$)	MSE	MAPE (%)	
ANN, Genetic Programming (GP) [38]	1 h	1.613, 2.142	1.146, 1.629	–	–	Australia
ANN [39]	1 h	–	–	–	3.288	Turkey (Mersin)
SVR [40]	1 h	2.5243	–	–	–	Iran
Empirical [41]	1 h	2.522	–	–	16.078	Mexico (Yucatan Peninsula/Calakmut)
RF-FFA [24]	1 h	18.9797	–	–	6.3826	Malaysia
Generalized Models [42]	1 h	1.7925	1.3800	–	–	India
ANFIS [18]	1 h	1.0482	–	–	4.6402	Iran
SVM-FFA [43]	1 h	0.6988	–	–	6.1768	Nigeria
MLFFNN [44]	1 h	0.3214 ($kWh/m^2/day$)	0.2531	0.1033 ($kWh/m^2/day$)	3.316	Iran
ANFIS, ANFIS-PSO, ANFIS-GA, ANFIS-DE [45]	1 h	0.3712, 0.3121, 0.3285, 0.3765	–	–	–	Malaysia
BPNN-PSO (Proposed Model)	5 s, 1 min	**0.1911, 0.2032**	**0.1000, 0.0956**	**0.0004, 0.0004**	**0.7484, 1.1271**	**Malaysia**

6. Conclusions

This paper has presented a hybrid prediction model using BPNN based PSO for the enhancement the GSR prediction performance. Two profiles, 3-days and 1-day have been investigated during training and validation process. The main contribution of this paper is developing a robust and consistent BPNN-PSO model for prediction of global solar irradiance at tropical country like Malaysia in extremely short-time intervals. Secondly, the implementation of PSO algorithm has significantly enhanced the classical BPNN architecture, by finding the optimal values of the architecture parameters, namely, hidden layers, neurons, and learning rate. The performance results of the proposed BPNN-PSO model have been compared with other widely used neural network models. Statistical error indicators RMSE, MAE, MSE, and MAPE have been used for performance and precision evaluation of all models. When the proposed model is used to predict solar irradiance based on the dataset of one region in Malaysia, the developed model has shown remarkable prediction improvements, proving that the model is superior to other techniques in terms of reliability, adaptability, and accurate correlation in GSR prediction of fast, short-time intervals, and nonlinear nature. From the results obtained, the 3-days profile performance evaluation of the BPNN-PSO are 1.7078 of RMSE, 0.7537 of MAE, 0.0292 of MSE, and 31.4348 of MAPE (%), at 5-s time interval, whereas the obtained results of 1-min interval are 0.6566 of RMSE, 0.2754 of MAE, 0.0043 of MSE, and 1.4732 of MAPE (%). In contrast,

the 1-day profile performance evaluation of the proposed method are 0.1911 of RMSE, 0.1000 of MAE, 0.0004 of MSE, and 0.7484 of MAPE (%), at 5-s time interval, whereas the obtained results of 1-min interval are 0.2032 of RMSE, 0.0956 of MAE, 0.0004 of MSE, and 1.1271 of MAPE (%). Even with the high accuracy performance of the model in different time intervals, the high performance is restricted to the availability of the aforementioned meteorological parameters. Moreover, the execution of the model needs to be extended to include spatial database using the proposed model for GSR prediction in short-time intervals. In addition, the optimization and calibration of the model could be proposed for the future work to make the model adaptable in different world regions.

Author Contributions: Conceptualization, A.A. and V.G.A.; methodology, A.A.; simulation, A.A.; validation, A.A. and N.M.L.T.; resources, H.S.; writing—original draft preparation, A.A., N.M.L.T., and V.G.A.; writing—review and editing, A.A., N.M.L.T., and V.G.A.; supervision, N.M.L.T.; project administration, N.M.L.T.; funding acquisition, N.M.L.T. All authors have read and agreed to the published version of the manuscript.

Funding: The authors would like to acknowledge the financial support received from Universiti Tenaga Nasional, Malaysia, BOLD Research Grant 2020 (BOLD 2020), Project Code: RJO10517844/110.

Data Availability Statement: No new data were created or analyzed in this study. Data sharing is not applicable to this article.

Conflicts of Interest: The authors declare no conflict of interest.

Abbreviations

GSR	Global solar irradiance
BPNN	Backpropagation neural network
PSO	Particle swarm optimization
PV	Photovoltaics
ANN	Artificial neural network
ANFIS	Adaptive neural-fuzzy inference system
MLFFNN	Multilayer feedforward neural network
MLP-NN	Multilayer perception neural network
MAE	Mean absolute error
GR-NN	Generalized regression neural network
RBF-NN	Radial basis function neural network
RMSE	Root mean square error

References

1. Jung, S.; Yoon, Y.T. Optimal Operating Schedule for Energy Storage System: Focusing on Efficient Energy Management for Microgrid. *Processes* **2019**, *7*, 80. [CrossRef]
2. Zhou, Y.; Wang, D.; Liu, Y.; Liu, J. Diffuse solar radiation models for different climate zones in China: Model evaluation and general model development. *Energy Convers. Manag.* **2019**, *185*, 518–536. [CrossRef]
3. Verbois, H.; Huva, R.; Rusydi, A.; Walsh, W. Solar irradiance forecasting in the tropics using numerical weather prediction and statistical learning. *Sol. Energy* **2018**, *162*, 265–277. [CrossRef]
4. Wang, Z.; Tian, C.; Zhu, Q.; Huang, M. Hourly Solar Radiation Forecasting Using a Volterra-Least Squares Support Vector Ma-chine Model Combined with Signal Decomposition. *Energies* **2018**, *11*, 68. [CrossRef]
5. Liu, Y.; Zhou, Y.; Chen, Y.; Wang, D.; Wang, Y.; Zhu, Y. Comparison of support vector machine and copula-based nonlinear quan-tile regression for estimating the daily diffuse solar radiation: A case study in China. *Renew. Energy* **2020**, *146*, 1101–1112. [CrossRef]
6. El Mghouchi, Y.; Chham, E.; Zemmouri, E.; El Bouardi, A. Assessment of different combinations of meteorological parameters for predicting daily global solar radiation using artificial neural networks. *Build. Environ.* **2019**, *149*, 607–622. [CrossRef]
7. Marzouq, M.; Bounoua, Z.; El Fadili, H.; Mechaqrane, A.; Zenkouar, K.; Lakhliai, Z. New daily global solar irradiation estimation model based on automatic selection of input parameters using evolutionary artificial neural networks. *J. Clean. Prod.* **2019**, *209*, 1105–1118. [CrossRef]
8. Wang, F.; Xuan, Z.; Zhen, Z.; Li, K.; Wang, T.; Shi, M. A day-ahead PV power forecasting method based on LSTM-RNN model and time correlation modification under partial daily pattern prediction framework. *Energy Convers. Manag.* **2020**, *212*, 112766. [CrossRef]

9. Jadidi, A.; Menezes, R.J.A.; De Souza, N.; Lima, A.D.C. A Hybrid GA–MLPNN Model for One-Hour-Ahead Forecasting of the Global Horizontal Irradiance in Elizabeth City, North Carolina. *Energies* **2018**, *11*, 2641. [CrossRef]
10. Jiang, H. A novel approach for forecasting global horizontal irradiance based on sparse quadratic RBF neural network. *Energy Convers. Manag.* **2017**, *152*, 266–280. [CrossRef]
11. Lotfinejad, M.M.; Hafezi, R.; Khanali, M.; Hosseini, S.S.; Mehrpooya, M.; Shamshirband, S. A Comparative Assessment of Predicting Daily Solar Radiation Using Bat Neural Network (BNN), Generalized Regression Neural Network (GRNN), and Neuro-Fuzzy (NF) System: A Case Study. *Energies* **2018**, *11*, 1188. [CrossRef]
12. Ghimire, S.; Deo, R.C.; Downs, N.J.; Raj, N. Self-adaptive differential evolutionary extreme learning machines for long-term solar radiation prediction with remotely-sensed MODIS satellite and Reanalysis atmospheric products in solar-rich cities. *Remote Sens. Environ.* **2018**, *212*, 176–198. [CrossRef]
13. Ghimire, D.; Raj, M. Deep Learning Neural Networks Trained with MODIS Satellite-Derived Predictors for Long-Term Global Solar Radiation Prediction. *Energies* **2019**, *12*, 2407. [CrossRef]
14. Dong, N.; Chang, J.-F.; Wu, A.-G.; Gao, Z.-K. A novel convolutional neural network framework based solar irradiance prediction method. *Int. J. Electr. Power Energy Syst.* **2020**, *114*, 105411. [CrossRef]
15. Wang, L.; Kisi, O.; Zounemat-Kermani, M.; Salazar, G.A.; Zhu, Z.; Gong, W. Solar radiation prediction using different techniques: Model evaluation and comparison. *Renew. Sustain. Energy Rev.* **2016**, *61*, 384–397. [CrossRef]
16. Elsheikh, A.H.; Sharshir, S.W.; Elaziz, M.A.; Kabeel, A.E.; Guilan, W.; Zhang, H. Modeling of solar energy systems using artificial neural network: A comprehensive review. *Sol. Energy* **2019**, *180*, 622–639. [CrossRef]
17. Meenal, R.; Selvakumar, A.I. Assessment of SVM, empirical and ANN based solar radiation prediction models with most influencing input parameters. *Renew. Energy* **2018**, *121*, 324–343. [CrossRef]
18. Mohammadi, K.; Shamshirband, S.; Tong, C.W.; Alam, K.A.; Petković, D. Potential of adaptive neuro-fuzzy system for prediction of daily global solar radiation by day of the year. *Energy Convers. Manag.* **2015**, *93*, 406–413. [CrossRef]
19. Wu, L.; Huang, G.; Fan, J.; Zhang, F.; Wang, X.; Zeng, W. Potential of kernel-based nonlinear extension of Arps decline model and gradient boosting with categorical features support for predicting daily global solar radiation in humid regions. *Energy Convers. Manag.* **2019**, *183*, 280–295. [CrossRef]
20. Khosravi, A.; Koury, R.; Machado, L.; Pabon, J. Prediction of hourly solar radiation in Abu Musa Island using machine learning algorithms. *J. Clean. Prod.* **2018**, *176*, 63–75. [CrossRef]
21. Fan, J.; Wu, L.; Zhang, F.; Cai, H.; Zeng, W.; Wang, X.; Zou, H. Empirical and machine learning models for predicting daily global solar radiation from sunshine duration: A review and case study in China. *Renew. Sustain. Energy Rev.* **2019**, *100*, 186–212. [CrossRef]
22. Bayrakçı, H.C.; Demircan, C.; Keçebaş, A. The development of empirical models for estimating global solar radiation on horizontal surface: A case study. *Renew. Sustain. Energy Rev.* **2018**, *81*, 2771–2782. [CrossRef]
23. Wang, H.; Liu, Y.; Zhou, B.; Li, C.; Cao, G.; Voropai, N.; Barakhtenko, E. Taxonomy research of artificial intelligence for deterministic solar power forecasting. *Energy Convers. Manag.* **2020**, *214*, 112909. [CrossRef]
24. Ibrahim, I.A.; Khatib, T. A novel hybrid model for hourly global solar radiation prediction using random forests technique and firefly algorithm. *Energy Convers. Manag.* **2017**, *138*, 413–425. [CrossRef]
25. Hocaoglu, F.O.; Serttaş, F. A novel hybrid (Mycielski-Markov) model for hourly solar radiation forecasting. *Renew. Energy* **2017**, *108*, 635–643. [CrossRef]
26. Ji, W.; Chee, K.C. Prediction of hourly solar radiation using a novel hybrid model of ARMA and TDNN. *Sol. Energy* **2011**, *85*, 808–817. [CrossRef]
27. Zang, H.; Cheng, L.; Ding, T.; Cheung, K.W.; Wang, M.; Wei, Z.; Sun, G. Estimation and validation of daily global solar radiation by day of the year-based models for different climates in China. *Renew. Energy* **2019**, *135*, 984–1003. [CrossRef]
28. Aybar-Ruiz, A.; Jiménez-Fernández, S.; Cornejo-Bueno, L.; Casanova-Mateo, C.; Sanz-Justo, J.; Salvador-González, P.; Salcedo-Sanz, S. A novel Grouping Genetic Algorithm–Extreme Learning Machine approach for global solar radiation prediction from numerical weather models inputs. *Sol. Energy* **2016**, *132*, 129–142. [CrossRef]
29. Qazi, A.; Fayaz, H.; Wadi, A.; Raj, R.G.; Rahim, N.; Khan, W.A. The artificial neural network for solar radiation prediction and designing solar systems: A systematic literature review. *J. Clean. Prod.* **2015**, *104*, 1–12. [CrossRef]
30. Alsina, E.F.; Bortolini, M.; Gamberi, M.; Regattieri, A. Artificial neural network optimisation for monthly average daily global solar radiation prediction. *Energy Convers. Manag.* **2016**, *120*, 320–329. [CrossRef]
31. Premalatha, N.; Arasu, A.V. Prediction of solar radiation for solar systems by using ANN models with different back propagation algorithms. *J. Appl. Res. Technol.* **2016**, *14*, 206–214. [CrossRef]
32. Yadav, A.K.; Chandel, S. Solar radiation prediction using Artificial Neural Network techniques: A review. *Renew. Sustain. Energy Rev.* **2014**, *33*, 772–781. [CrossRef]
33. Mohandes, M.A. Modeling global solar radiation using Particle Swarm Optimization (PSO). *Sol. Energy* **2012**, *86*, 3137–3145. [CrossRef]
34. Ghazvinian, H.; Mousavi, S.-F.; Karami, H.; Farzin, S.; Ehteram, M.; Hossain, S.; Fai, C.M.; Bin Hashim, H.; Singh, V.P.; Ros, F.C.; et al. Integrated support vector regression and an improved particle swarm optimization-based model for solar radiation prediction. *PLoS ONE* **2019**, *14*, e0217634. [CrossRef]

35. Ehteram, M.; Ahmed, A.N.; Chow, M.F.; Afan, H.A.; El-Shafie, A. Accuracy Enhancement for Zone Mapping of a Solar Radiation Forecasting Based Multi-Objective Model for Better Management of the Generation of Renewable Energy. *Energies* **2019**, *12*, 2730. [CrossRef]
36. Malvoni, M.; Hatziargyriou, N. One-day ahead PV power forecasts using 3D Wavelet Decomposition. In Proceedings of the 2019 International Conference on Smart Energy Systems and Technologies (SEST), Porto, Portugal, 9–11 September 2019; pp. 1–6.
37. Zou, L.; Wang, L.; Xia, L.; Zou, L.; Hu, B.; Zhu, H. Prediction and comparison of solar radiation using improved empirical models and Adaptive Neuro-Fuzzy Inference Systems. *Renew. Energy* **2017**, *106*, 343–353. [CrossRef]
38. Ghimire, S.; Deo, R.C.; Downs, N.J.; Raj, N. Global solar radiation prediction by ANN integrated with European Centre for medium range weather forecast fields in solar rich cities of Queensland Australia. *J. Clean. Prod.* **2019**, *216*, 288–310. [CrossRef]
39. Çelik, Ö.; Teke, A.; Yıldırım, H.B. The optimized artificial neural network model with Levenberg–Marquardt algorithm for global solar radiation estimation in Eastern Mediterranean Region of Turkey. *J. Clean. Prod.* **2016**, *116*, 1–12. [CrossRef]
40. Shamshirband, S.; Mohammadi, K.; Chen, H.-L.; Samy, G.N.; Petković, D.; Ma, C. Daily global solar radiation prediction from air temperatures using kernel extreme learning machine: A case study for Iran. *J. Atmospheric Solar-Terrestrial Phys.* **2015**, *134*, 109–117. [CrossRef]
41. Quej, V.H.; Almorox, J.; Ibrakhimov, M.; Saito, L. Empirical models for estimating daily global solar radiation in Yucatán Peninsula, Mexico. *Energy Convers. Manag.* **2016**, *110*, 448–456. [CrossRef]
42. Anis, S.; Jamil, B.; Ansari, A.; Bellos, E. Generalized models for estimation of global solar radiation based on sunshine duration and detailed comparison with the existing: A case study for India. *Sustain. Energy Technol. Assess.* **2019**, *31*, 179–198. [CrossRef]
43. Olatomiwa, L.; Mekhilef, S.; Shamshirband, S.; Mohammadi, K.; Petković, D.; Sudheer, C. A support vector machine–firefly algorithm-based model for global solar radiation prediction. *Sol. Energy* **2015**, *115*, 632–644. [CrossRef]
44. Khosravi, A.; Nunes, R.; Assad, M.E.H.; Machado, L. Comparison of artificial intelligence methods in estimation of daily global solar radiation. *J. Clean. Prod.* **2018**, *194*, 342–358. [CrossRef]
45. Halabi, L.M.; Mekhilef, S.; Hossain, M. Performance evaluation of hybrid adaptive neuro-fuzzy inference system models for predicting monthly global solar radiation. *Appl. Energy* **2018**, *213*, 247–261. [CrossRef]